



**HAL**  
open science

## Quantification of Lambda ( $\Lambda$ ) in multi-elemental compound-specific isotope analysis

Patrick Höhener, Gwenael Imfeld

► **To cite this version:**

Patrick Höhener, Gwenael Imfeld. Quantification of Lambda ( $\Lambda$ ) in multi-elemental compound-specific isotope analysis. *Chemosphere*, 2021, 267, pp.129232. 10.1016/j.chemosphere.2020.129232 . hal-03082804

**HAL Id: hal-03082804**

**<https://amu.hal.science/hal-03082804v1>**

Submitted on 18 Dec 2020

**HAL** is a multi-disciplinary open access archive for the deposit and dissemination of scientific research documents, whether they are published or not. The documents may come from teaching and research institutions in France or abroad, or from public or private research centers.

L'archive ouverte pluridisciplinaire **HAL**, est destinée au dépôt et à la diffusion de documents scientifiques de niveau recherche, publiés ou non, émanant des établissements d'enseignement et de recherche français ou étrangers, des laboratoires publics ou privés.

# 1 Quantification of Lambda ( $\Lambda$ ) in multi-elemental compound- 2 specific isotope analysis

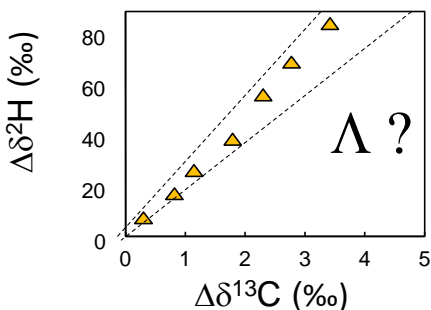
3 <sup>1</sup>Patrick Höhener\* and <sup>2</sup>Gwenaél Imfeld

4 <sup>1</sup>Aix Marseille University – CNRS, UMR 7376, Laboratory of Environmental Chemistry,  
5 Marseille, France, Phone No. 0033413551034

6 \*Corresponding author. patrick.hohener@univ-amu.fr

7 <sup>2</sup>Laboratory of Hydrology and Geochemistry of Strasbourg (LHyGeS), Université de  
8 Strasbourg, UMR 7517 CNRS/EOST, 1 Rue Blessig, 67084, Strasbourg Cedex, France

9 *Short communication to Chemosphere, <https://doi.org/10.1016/j.chemosphere.2020.129232>*



10

---

## 11 Highlights

12 The parameter  $\Lambda$  represents dual element stable isotope data

13 Two conventions for quantifying  $\Lambda$  give different  $\Lambda$  values

14 Linear regressions of delta values in a dual element plot overestimate  $\Lambda$

15 We show that only the ln-transformed isotope ratios should be fitted

16

17

**18 ABSTRACT**

19 In multi-elemental compound-specific isotope analysis the lambda ( $\Lambda$ ) value expresses the  
20 isotope shift of one element versus the isotope shift of a second element. In dual-isotope plots,  
21 the slope of the regression lines typical reveals the footprint of the underlying isotope effects  
22 allowing to distinguish degradation pathways of an organic contaminant molecule in the  
23 environment. While different conventions and fitting procedures are used in the literature to  
24 determine  $\Lambda$ , it remains unclear how they affect the magnitude of  $\Lambda$ . Here we generate synthetic  
25 data for benzene  $\delta^2\text{H}$  and  $\delta^{13}\text{C}$  with two enrichment factors  $\varepsilon_H$  and  $\varepsilon_C$  using the Rayleigh equation  
26 to examine how different conventions and linear fitting procedures yield distinct  $\Lambda$ . Fitting an  
27 error-free data set in a graph plotting the  $\delta^2\text{H}$  versus  $\delta^{13}\text{C}$  overestimates  $\Lambda$  by  $0.225\% \cdot \varepsilon_H/\varepsilon_C$ ,  
28 meaning that if  $\varepsilon_H/\varepsilon_C$  is larger than 22,  $\Lambda$  is overestimated by more than 5%. The correct fitting  
29 of  $\Lambda$  requires a natural logarithmic transformation of  $\delta^2\text{H}$  versus  $\delta^{13}\text{C}$  data. Using this  
30 transformation, the ordinary linear regression (OLR), the reduced major-axis (RMA) and the  
31 York methods find the correct  $\Lambda$ , even for large  $\varepsilon_H/\varepsilon_C$ . Fitting a dataset with synthetic data with  
32 typical random errors let to the same conclusion and positioned the suitability of each regression  
33 method. We conclude that fitting of non-transformed  $\delta$  values should be discontinued. The  
34 validity of most previous  $\Lambda$  values is not compromised, although previously obtained  $\Lambda$  values  
35 for large  $\varepsilon_H/\varepsilon_C$  could be corrected using our error estimation to improve comparison.

**36 Key Words**

37 Stable isotopes, pollution, assessment, bioremediation

## 38 1. Introduction

39 Multi-elemental Compound-Specific Isotope Analysis (ME-CSIA) is increasingly used to assess  
40 the fate of pollutants such as hydrocarbons (Vogt et al., 2016), chlorinated solvents solvents  
41 (Palau et al., 2014, Audi-Miro et al., 2015, Palau et al., 2016), nitrates (Xue et al., 2009),  
42 perchlorates (Sturchio et al., 2012) and pesticides (Ponsin et al., 2019, Melsbach et al., 2020) in  
43 the environment. The slope of the dual-isotope plot (Lambda,  $\Lambda$ ) reflects changes of the isotope  
44 ratios of each element, which can be specific to a reaction mechanism, and thus inform about  
45 transformation processes in the laboratory or in the field. (Vogt et al., 2016, Elsner, 2010)  
46 Several studies (Masbou et al., 2018, Huntscha et al., 2014, Lian et al., 2019, Bouchard et al.,  
47 2018, Vogt et al., 2016, Elsner, 2010, Ojeda et al., 2019) refer to  $\Lambda$  using the simple definition in  
48 eq. 1, which is written here as an example for hydrogen vs carbon  $\delta$  values (eq. 1).

$$49 \Lambda = \frac{\Delta\delta^{2H}}{\Delta\delta^{13C}} \approx \frac{\epsilon_H}{\epsilon_C} \quad \text{eq. 1}$$

50 where  $\Delta\delta$  is the change of isotope ratios from initial values, and  $\epsilon$  are the enrichment factors for  
51 hydrogen and carbon. The Lambda ( $\Lambda$ ) is an important parameter in ME-CSIA. It is a practical  
52 and unitless number which characterizes a specific process. It can be determined either by simply  
53 using the two enrichment factors and the right-hand side of equation 1 on one hand, or from  
54 regression analysis in a dual-isotope plots with isotope data of one element versus data of  
55 another element in the same compound (Figure 1). Lambda values were obtained in many studies  
56 (Ojeda et al., 2019, Palau et al., 2017, Rosell et al., 2007, Rodriguez-Fernandez et al., 2018,  
57 Rodriguez-Fernandez et al., 2018, Dogan-Subasi et al., 2017, Cretnik et al., 2013, Audi-Miro et  
58 al., 2013, Palau et al., 2014, Lian et al., 2019, Badin et al., 2016, Mogusu et al., 2015, Ponsin et

59 al., 2019, McKelvie et al., 2009, Pati et al., 2012) from the regression analyses in dual-isotope  
60 plots (i.e., ratios of one isotope as a function of another isotope as delta values; Figure 1A).

61 Another mathematical notation for  $\Lambda$  has been described in detail in (Wijker et al., 2013) (eq. 2),  
62 noted here for hydrogen and carbon isotopes:

$$63 \quad \Lambda = \frac{\ln\left[\frac{(\delta^{2H}/1000 + 1)}{(\delta^{2H_0}/1000 + 1)}\right]}{\ln\left[\frac{(\delta^{13C}/1000 + 1)}{(\delta^{13C_0}/1000 + 1)}\right]} \approx \frac{\varepsilon_H}{\varepsilon_C} \quad \text{eq. 2}$$

64 Figure 1B shows an example of a dual-isotope plot to determine  $\Lambda$  using eq. 2, named below the  
65 ln-transformed  $\delta$  data. This way of obtaining  $\Lambda$  was used e.g. in ( Schilling et al., 2019 a+b).

66 Apart from those two different conventions for plotting isotope data, different methods of linear  
67 regression were proposed to obtain  $\Lambda$ . These include the ordinary linear regression (OLR), the  
68 reduced major axis regression (RMA), and the York linear regression, which have been  
69 compared recently (Ojeda et al., 2019).

70 The objective of this short comment is to compare the two conventions (i.e., A, with eq. 1 and B,  
71 with 2) to determine  $\Lambda$  values and the associated uncertainty from a dual-isotope plot. Two  
72 synthetic datasets were generated, one without random error, and a second one with random  
73 errors mimicking measurement uncertainties. Each dataset was fitted with the ordinary linear  
74 regression (OLR), the reduced major-axis (RMA) and the York regression methods and results  
75 were compared.

## 76 **2. Methods**

77 The Rayleigh equation (eq. 3) (Aelion et al., 2010) was used to generate 10 synthetic exact data  
78 points for each element (i.e., C and H). We used isotope enrichment factors for carbon and

79 hydrogen corresponding to methanogenic degradation of benzene:  $\epsilon_C = -2.0$  and  $\epsilon_H = -59.5$  ‰.  
80 (Mancini et al., 2003) The remaining fraction ( $f$ ) of benzene was varied from 1 to 0.1 in steps of  
81 0.1 (see data set in the supplementary data).

$$82 \quad \frac{R}{R_0} = f^{(\alpha-1)} \quad \text{eq. 3}$$

83 Where  $R$  is the isotope ratio,  $R_0$  is the initial isotope ratio (chosen as the  $R$  of international  
84 standard  $R_{\text{std}}$ ),  $f$  is the fraction of compound remaining ( $C/C_0$ ), and  $\alpha$  is the isotope fractionation  
85 factor (equal to  $\epsilon/1000 + 1$ ). The resulting isotope ratios were expressed as  $\delta$  values [ $\delta = (R/R_{\text{std}} -$   
86  $1) * 1000$ ;  $R_{\text{std,H}} = 1.5575\text{E-}4$ ;  $R_{\text{std,C}} = 0.011237$ ] and plotted in Figure 1A ( $\Delta\delta^2\text{H}$  vs  $\Delta\delta^{13}\text{C}$ , eq. 1)  
87 and 1B (ln-transformed data, eq. 2). The resulting slopes should reflect the ratio of original  
88 isotopic enrichment values,  $-59.50/-2.00$ , thus  $\Lambda = 29.75$ .

89 A second dataset was generated using the same enrichment factors but introducing random errors  
90 in the calculated  $\delta$  values (see Table S1 in supplementary data). The  $\delta$  values of this set had a  
91 random error of up to  $\pm 0.5$  ‰ for carbon and up to  $\pm 5.0$  ‰ for hydrogen, which corresponds to  
92 the typical total analytical uncertainties.

93 Finally, 25 more datasets (data not shown) were generated in the same manner as dataset 1  
94 without random error, keeping  $\epsilon_C = -2.0$  ‰ and varying  $\epsilon_H$  over  $\epsilon_H / \epsilon_C$  ratios from 2 to 50. Each  
95 of these data sets was fitted with OLR, and the overestimation of fit A over fit B was quantified  
96 and plotted in Figure 2 as a function of  $\epsilon_H / \epsilon_C$ .

97 The datasets were generated with Excel (Microsoft), Vs. 2011), and linear regressions (OLR,  
98 RMA and York) were calculated with a script adapted from Ojeda et al. (2019) and were not  
99 forced through the origin.

### 100 3. Results

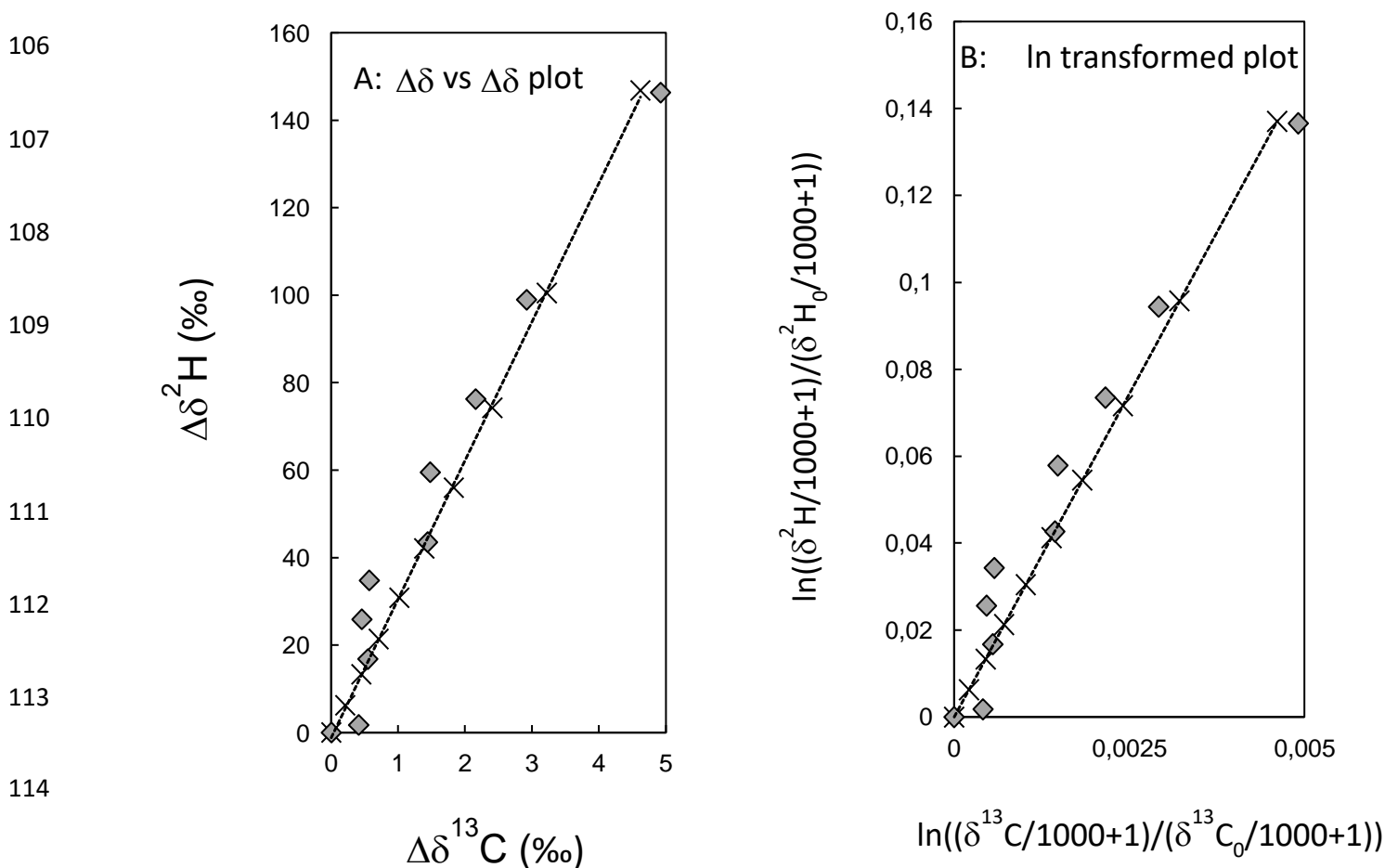
101 The dataset 1 with the raw  $\Delta\delta$  values (eq. 1) does not plot on a perfect straight line (Figure 1A).

102 The slope becomes steeper with increasing  $\delta$  values (smaller  $f$ ). An OLR gives a mean  $\Lambda$  of

103  $31.70 \pm 0.21$  ( $R^2 > 0.99$ ), which overestimates the true  $\Lambda$  of 29.75 by 6.6 %. In contrast, the

104 dataset 1 with ln-transformed  $\delta$  values (eq. 2) plots perfectly on a straight line with a slope of

105  $29.74 \pm 0.02$  with an  $R^2$  of 1.0000 (Figure 1B), which matches the true  $\Lambda$ .



115 **Fig. 1.** Dual-isotope plot of A) raw  $\Delta\delta$  values (according to eq. 1), and B) ln-transformed  $\delta$

116 values (according to eq. 2). Crosses correspond to exact datapoints (dataset 1) and grey

117 diamonds are datapoints with random error (dataset 2).

118

119 **Table 1:** Comparison of  $\Lambda$  calculated with the raw  $\Delta\delta$  values (convention A, eq. 1) and the  $\ln$ -transformed  $\delta$  values (convention B, eq.  
 120 2) using the OLR, RMA and York methods, for the exact data points (dataset 1) and data generated with a random error (dataset 2).

121

127

<i>Exact data points (dataset 1)</i>							<i>Random error (dataset 2)</i>					
<i><math>\Delta\delta</math> vs <math>\Delta\delta</math></i>				<i><math>\ln</math>-transformed</i>			<i><math>\Delta\delta</math> vs <math>\Delta\delta</math></i>			<i><math>\ln</math>-transformed</i>		
	<i><math>\Lambda</math></i>	<i>SE</i>	<i><math>R^2</math></i>	<i><math>\Lambda</math></i>	<i>SE</i>	<i><math>R^2</math></i>	<i><math>\Lambda</math></i>	<i>SE</i>	<i><math>R^2</math></i>	<i><math>\Lambda</math></i>	<i>SE</i>	<i><math>R^2</math></i>
<i>OLR</i>	31.70	0.21	>0.99	29.74	0.02	1.00	30.08	2.13	0.96	28.15	2.16	0.95
<i>RMA</i>	31.71	0.19	>0.99	29.74	0.02	1.00	30.67	1.90	0.98	28.80	1.93	0.98
<i>York</i>	31.71	3.77	>0.99	29.74	3.56	1.00	31.17	3.68	0.96	29.33	3.50	0.95

122 *SE: Standard error of  $\Lambda$* 

128

123

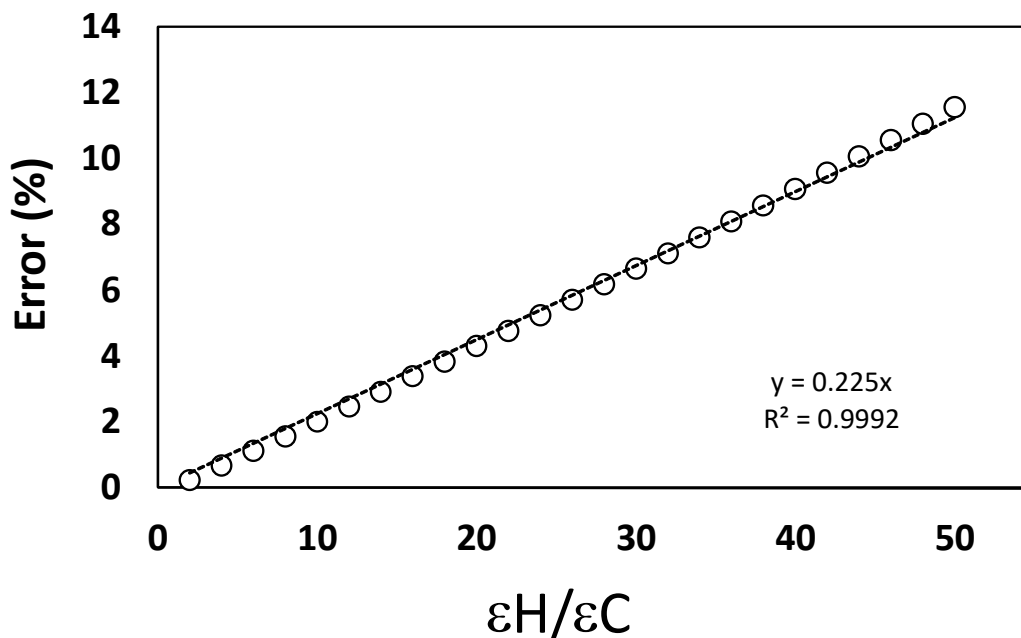
124

125

126



129 The overestimation of  $\Lambda$  calculated with convention A compared to convention B was quantified  
130 as a function of  $\varepsilon_H/\varepsilon_C$  ranging from 2 to 50 (Fig. 2; OLR method)).



131

132 **Fig. 2** Overestimation of  $\Lambda$  (%) as a function of  $\varepsilon_H/\varepsilon_C$  (symbols) when convention A (eq. 1) is  
133 used. The straight dotted line is the mean error increase of 0.225% per  $\varepsilon_H/\varepsilon_C$ .

134 Figure 2 shows that the error in a graph plotting the  $\delta$  values like in Fig. 1.A overestimates  $\Lambda$  by  
135 11.5 % when  $\varepsilon_H/\varepsilon_C$  reaches 50. The increase of the error is almost linear with a slope of 0.225%  
136 per  $\varepsilon_H/\varepsilon_C$ .

#### 137 4. Discussion

138 The use of the exact (error-free) synthetic dataset to compare conventions A (eq. 1) and B (eq. 2)  
139 emphasized that  $\Lambda$  calculated with convention A is linearly overestimated (eq.1). The difference

140 of  $\Lambda$  obtained with convention A and B has a pure mathematical cause (Wijker et al., 2013):  
141 equation 1 is derived from eq. 2 by a Taylor series expansion which is only approximate.

142 Höhener and Atteia (Höhener and Atteia, 2014) derived mathematically the dependence of the  
143 slope  $\Lambda$  on the remaining, non-degraded fraction  $f$  in a dual-isotope plot (eq. 4) based on the  
144 theory of Rayleigh distillation.

$$145 \quad \Lambda = \frac{\Delta\delta^{2H}}{\Delta\delta^{13C}} = \frac{f^{\frac{\epsilon_H}{1000}-1}}{f^{\frac{\epsilon_C}{1000}-1}} \quad \text{eq. 4}$$

146 Equation 4 (eq. 16 in (Höhener and Atteia, 2014)) shows that  $\Lambda$  is increasing with decreasing  $f$ ,  
147 as observed in Figure 1A. Thus, for  $f$  close to one,  $\Lambda$  is 29.75, while for  $f = 0.1$ ,  $\Lambda$  is 31.80.

148 All three regression methods tested for convention A with dataset 1 gave a similar  $\Lambda$  of 31.7,  
149 although their standard errors (SE) differed (Table 1). OLR and RMA methods gave a narrow SE  
150 (0.21 and 0.19, respectively), leading us to the wrong conclusion that  $\Lambda$  is  $> 31$ . Regression with  
151 the York method gave a larger SE ( $\Lambda = 31.71 \pm 3.68$ , Tab. 1), which represents a correct but  
152 inaccurate description of the true  $\Lambda$  of 29.75. For convention B and dataset 1, all three regression  
153 methods find the true  $\Lambda$ , although only the OLR and RMA method yielded accurate  $\Lambda$  within  
154 narrow error limits.

155 Measured isotope ratios are always affected by random errors from measurements, which were  
156 accounted for in dataset 2 to calculate  $\Lambda$  (Table 1). All three methods predicted  $\Lambda > 31$  using  
157 convention A, and  $\Lambda$  was associated with large SE, ranging from 1.90 to 3.68. Using convention  
158 B,  $\Lambda$  ranged from 28.15 to 29.33, with SE ranging from 1.9 (RMA) to 3.5 (York). For dataset 2,  
159 RMA was the best fitting method, yielding the narrower SE, while both OLR and York gave

160 accurate predictions also with higher error. All regressions match thus the true value of 29.75  
161 within their error limits.

162 To sum up, the error-free data in a dual-isotope plot with  $\Delta\delta$  vs  $\Delta\delta$  values do not lie on a straight  
163 line and thus should not be fitted with any linear regression. The slope in a  $\Delta\delta$  vs  $\Delta\delta$  plot is per  
164 definition a function of the progress of reaction  $f$  (eq. 4). A non-linear curve is obtained,  
165 especially when the orders of magnitude of the enrichment factors differ. Linear regressions in  
166 such plots yield  $\Lambda$  that overestimate the true  $\Lambda$  and should be discontinued. The correct  
167 convention to linearize data is provided in eq. 2 and should be applied as in Figure 1B to obtain  
168 accurate  $\Lambda$ . OLR and RMA regression methods yield narrower error estimates, whereas the York  
169 method finds the true  $\Lambda$  within a larger error margin. The validity of most previously obtained  $\Lambda$   
170 values with convention A might not be compromised given the total uncertainty of the  
171 experimental and analytical methods. However, in a few cases with large  $\varepsilon_H/\varepsilon_C$  ratios, corrections  
172 might be applied in order to compare optimally all  $\Lambda$  values. The simple procedure to follow  
173 consists in using Fig. 2 of our manuscript, selecting the appropriate ratio of epsilons, reporting  
174 the corresponding error percentage (which is the percentage of overestimation) to lower  $\Lambda$  by this  
175 percentage. Worthy of note, if experimental data still plotting nonlinearly on a ln-transformed  
176 plot with eq. 2, as e.g. in (Dorer et al., 2014), another process may be involved, including a very  
177 strong hydrogen fractionation (tunneling), concentration-dependent fractionation and/or  
178 instrumental non-linearity. In these specific cases,  $\Lambda$  cannot be expressed as a constant number.

## 179 **Acknowledgments**

180 This work is funded by the French National research Agency ANR through grant ANR-18-CE04-  
181 0004-01, project DECISIVE.

**182 Supplementary data**

183 Table of synthetic datasets used in this work.

184

185

**186 5. References**

187 Aelion, C. M., Höhener, P., Hunkeler, D., Aravena, R. Environmental Isotopes in Biodegradation  
188 and Bioremediation. CRC Press (Taylor and Francis), Boca Raton, 2010.

189 Audi-Miro, C., Cretnik, S., Otero, N., Palau, J., Shouakar-Stash, O., Soler, A., Elsner, M., 2013.  
190 Cl and C isotope analysis to assess the effectiveness of chlorinated ethene degradation by  
191 zero-valent iron: Evidence from dual element and product isotope values. Appl. Geochem.  
192 32, 175-183.

193 Audi-Miro, C., Cretnik, S., Torrento, C., Rosell, M., Shouakar-Stash, O., Otero, N., Palau, J.,  
194 Elsner, M., Soler, A., 2015. C, Cl and H compound-specific isotope analysis to assess  
195 natural versus Fe(0) barrier-induced degradation of chlorinated ethenes at a contaminated  
196 site. J. Hazard. Mat. 299, 747-754.

197 Badin, A., Broholm, M. M., Jacobsen, C. S., Palau, J., Dennis, P., Hunkeler, D., 2016.  
198 Identification of abiotic and biotic reductive dechlorination in a chlorinated ethene plume  
199 after thermal source remediation by means of isotopic and molecular biology tools. J.  
200 Contam. Hydrol. 192, 1-19.

- 201 Bouchard, D., Hunkeler, D., Madsen, E., Buscheck, T., Daniels, E., Kolhatkar, R., DeRito, C.,  
202 Aravena, R., Thomson, N., 2018. Application of Diagnostic Tools to Evaluate Remediation  
203 Performance at Petroleum Hydrocarbon-Impacted Sites. *Ground Wat. Monitor. Remed.* 38,  
204 88-98.
- 205 Cretnik, S., Thoreson, K. A., Bernstein, A., Ebert, K., Buchner, D., Laskov, C., Haderlein, S.,  
206 Shouakar-Stash, O., Kliegman, S., McNeill, K., Elsner, M., 2013. Reductive Dechlorination  
207 of TCE by Chemical Model Systems in Comparison to Dehalogenating Bacteria: Insights  
208 from Dual Element Isotope Analysis (C-13/C-12, Cl-37/Cl-35). *Environ. Sci. Technol.* 47,  
209 6855-6863.
- 210 Dogan-Subasi, E., Elsner, M., Qiu, S., Cretnik, S., Atashgahi, S., Shouakar-Stash, O., Boon, N.,  
211 Dejonghe, W., Bastiaens, L., 2017. Contrasting dual (C, Cl) isotope fractionation offers  
212 potential to distinguish reductive chloroethene transformation from breakdown by  
213 permanganate. *Sci. Tot. Environ.* 596, 169-177.
- 214 Dorer, C., Höhener, P., Hedwig, N., Richnow, H. H., Vogt, C., 2014. Rayleigh-based concept to  
215 tackle strong hydrogen fractionation in dual-isotope-analysis - the example of ethylbenzene  
216 degradation of *Aromatoleum aromaticum*. *Environ. Sci. Technol.* 48, 5788–5797.
- 217 Elsner, M., 2010. Stable isotope fractionation to investigate natural transformation mechanisms  
218 of organic contaminants: principles, prospects and limitations. *J. Environ. Monitoring* 12,  
219 2005-2031.
- 220 Huntscha, S., Hofstetter, T., Schymanski, E., Spahr, S., Hollender, J., 2014. Biotransformation of  
221 Benzotriazoles: Insights from Transformation Product Identification and Compound-  
222 Specific Isotope Analysis. *Environ. Sci. Technol.* 48, 4435-4443.

- 223 Höhener, P., Atteia, O., 2014. Rayleigh equation for evolution of stable isotope ratios in  
224 contaminant decay chains. *Geochim. Cosmochim. Acta* 126, 70-77.
- 225 Lian, S., Wu, L., Nikolausz, M., Lechtenfeld, O., Richnow, H., 2019. H-2 and C-13 isotope  
226 fractionation analysis of organophosphorus compounds for characterizing transformation  
227 reactions in biogas slurry: Potential for anaerobic treatment of contaminated biomass.  
228 *Water Res.* 163, 114882.
- 229 Mancini, S. A., Ulrich, A. C., Lacrampe-Couloume, G., Sleep, B., Edwards, E. A., Sherwood-  
230 Lollar, B., 2003. Carbon and Hydrogen Isotopic Fractionation during Anaerobic  
231 Biodegradation of Benzene. *Appl. Environ. Microbiol.* 69, 191-198.
- 232 Masbou, J., Drouin, G., Payraudeau, S., Imfeld, G., 2018. Carbon and nitrogen stable isotope  
233 fractionation during abiotic hydrolysis of pesticides. *Chemosphere* 213, 368-376.
- 234 McKelvie, J., Hyman, M., Elsner, M., Smith, C., Aslett, D., Lacrampe-Couloume, G., Sherwood  
235 Lollar, B., 2009. Isotopic Fractionation of Methyl tert-Butyl Ether Suggests Different Initial  
236 Reaction Mechanisms during Aerobic Biodegradation. *Environ. Sci. Technol.* 43, 2793-  
237 2799.
- 238 Melsbach, A., Torrento, C., Ponsin, V., Bolotin, J., Lachat, L., Prasuhn, V., Hofstetter, T.,  
239 Hunkeler, D., Elsner, M., 2020. Dual-Element Isotope Analysis of Desphenylchloridazon to  
240 Investigate Its Environmental Fate in a Systematic Field Study: A Long-Term Lysimeter  
241 Experiment. *Environ. Sci. Technol.* 54, 3929-3939.
- 242 Mogusu, E., Wolbert, J., Kujawinski, D., Jochmann, M., Elsner, M., 2015. Dual element (N-  
243 15/N-14, C-13/C-12) isotope analysis of glyphosate and AMPA by derivatization-gas

- 244 chromatography isotope ratio mass spectrometry (GC/IRMS) combined with LC/IRMS.  
245 Anal. Bioanal. Chem. 407, 5249-5260.
- 246 Ojeda, A., Phillips, E., Mancini, S., Sherwood Lollar, B., 2019. Sources of Uncertainty in  
247 Biotransformation Mechanistic Interpretations and Remediation Studies using CSIA. Anal.  
248 Chem. 91, 9147-9153.
- 249 Palau, J., Jamin, P., Badin, A., Vanhecke, N., Haerens, B., Brouyere, S., Hunkeler, D., 2016. Use  
250 of dual carbon-chlorine isotope analysis to assess the degradation pathways of 1,1,1-  
251 trichloroethane in groundwater. Water Res. 92, 235-243.
- 252 Palau, J., Shouakar-Stash, O., Hunkeler, D., 2014. Carbon and Chlorine Isotope Analysis to  
253 Identify Abiotic Degradation Pathways of 1,1,1-Trichloroethane. Environ. Sci. Technol. 48,  
254 14400-14408.
- 255 Palau, J., Yu, R., Mortan, S., Shouakar-Stash, O., Rosell, M., Freedman, D., Sbarbati, C.,  
256 Fiorenza, S., Aravena, R., Marco-Urrea, E., Elsner, M., Soler, A., Hunkeler, D., 2017.  
257 Distinct Dual C-C1 Isotope Fractionation Patterns during Anaerobic Biodegradation of 1,2-  
258 Dichloroethane: Potential To Characterize Microbial Degradation in the Field. Environ.  
259 Sci. Technol. 51, 2685-2694.
- 260 Pati, S., Shin, K., Skarpeli-Liati, M., Bolotin, J., Eustis, S., Spain, J., Hofstetter, T., 2012. Carbon  
261 and Nitrogen Isotope Effects Associated with the Dioxygenation of Aniline and  
262 Diphenylamine. Environ. Sci. Technol. 46, 11844-11853.

- 263 Ponsin, V., Torrento, C., Lihl, C., Elsner, M., Hunkeler, D., 2019. Compound-Specific Chlorine  
264 Isotope Analysis of the Herbicides Atrazine, Acetochlor, and Metolachlor. *Anal. Chem.* 91,  
265 14290-14298.
- 266 Rodriguez-Fernandez, D., Heckel, B., Torrento, C., Meyer, A., Elsner, M., Hunkeler, D., Soler,  
267 A., Rosell, M., Domenech, C., 2018. Dual element (C-Cl) isotope approach to distinguish  
268 abiotic reactions of chlorinated methanes by Fe(0) and by Fe(II) on iron minerals at neutral  
269 and alkaline pH. *Chemosphere* 206, 447-456.
- 270 Rosell, M., Barcelo, D., Rohwerder, T., Breuer, U., Gehre, M., Richnow, H. H., 2007. Variations  
271 in C-13/C-12 and D/H enrichment factors of aerobic bacterial fuel oxygenate degradation.  
272 *Environ. Sci. Technol.* 41, 2036-2043.
- 273 Schilling, I., Bopp, C., Lal, R., Kohler, H., Hofstetter, T., 2019a. Assessing Aerobic  
274 Biotransformation of Hexachlorocyclohexane Isomers by Compound-Specific Isotope  
275 Analysis. *Environ. Sci. Technol.* 53, 7419-7431.
- 276 Schilling, I., Hess, R., Bolotin, J., Lal, R., Hofstetter, T., Kohler, H., 2019b. Kinetic Isotope  
277 Effects of the Enzymatic Transformation of gamma-Hexachlorocyclohexane by the  
278 Lindane Dehydrochlorinase Variants LinA1 and LinA2. *Environ. Sci. Technol.* 53, 2353-  
279 2363.
- 280 Sturchio, N. C., Hoaglund, J. R., Marroquin, R. J., Beloso, A. D., Heraty, L. J., Bortz, S. E.,  
281 Patterson, T. L., 2012. Isotopic mapping of groundwater perchlorate plumes. *Ground Water*  
282 50, 94-102.



- 283 Vogt, C., Dorer, C., Musat, F., Richnow, H. H., 2016. Multi-element isotope fractionation  
284 concepts to characterize the biodegradation of hydrocarbons from enzymes to the  
285 environment. *Curr. Opin. Biotechnol.* 41, 90-98.
- 286 Wijker, R., Adamczyk, P., Bolotin, J., Paneth, P., Hofstetter, T., 2013. Isotopic Analysis of  
287 Oxidative Pollutant Degradation Pathways Exhibiting Large H Isotope Fractionation.  
288 *Environ. Sci. Technol.* 47, 13459-13468.
- 289 Xue, D., Botte, J., De Baets, B., Accoe, F., Nestler, A., Taylor, P., Van Cleemput, O., Berglund,  
290 M., Boeckx, P., 2009. Present limitations and future prospects of stable isotope methods for  
291 nitrate source identification in surface- and groundwater. *Water Res.* 43, 1159-1170.

292

293

294

295

296

297

298

299

300

301

302

303 **SUPPLEMENTARY DATA**304 **Quantification of Lambda ( $\Lambda$ ) in multi-elemental compound-specific isotope**  
305 **analysis**306 **<sup>1</sup>Patrick Höhener\* and <sup>2</sup>Gwenaël Imfeld**307 <sup>1</sup>Aix Marseille University – CNRS, UMR 7376, Laboratory of Environmental Chemistry, Marseille,  
308 France

309 \*Corresponding author. patrick.hohener@univ-amu.fr

310 <sup>2</sup>Laboratory of Hydrology and Geochemistry of Strasbourg (LHyGeS), Université de Strasbourg, UMR  
311 7517 CNRS/EOST, 1 Rue Blessig, 67084, Strasbourg Cedex, France312 **Contents:**313 **Table S1: Datasets used in this work**314 *Table S1: Synthetic data shown in Figure 1 and used for fitting.*

Remaining fraction f	Exact data points (dataset 1)		Random error (dataset 2)	
	$\delta^{13}\text{C}$ ‰	$\delta^2\text{H}$ ‰	$\delta^{13}\text{C}$ ‰	$\delta^2\text{H}$ ‰
1	0	0	0	0
0.9	0.21	6.29	0.41	1.79
0.8	0.45	13.37	0.55	16.87
0.7	0.71	21.45	0.46	25.95
0.6	1.02	30.86	0.57	34.86
0.5	1.39	42.10	1.44	43.6
0.4	1.83	56.03	1.48	59.53
0.3	2.41	74.26	2.16	76.26
0.2	3.22	100.50	2.92	99.0
0.1	4.62	146.83	4.92	146.33

315

316

317